Challenging Glass 5 – Conference on Architectural and Structural Applications of Glass
Belis, Bos & Louter (Eds.), Ghent University, June 2016.

ISBN 978-90-825-2680-6

Low Cost Double Curvature – Exploratory Computational Modelling, FE-analysis and Prototyping of Cold-Bent Glass

P. Eversmann [a], A. Ihde [b] & C. Louter [c]
[a] *ETH Zürich, Switzerland, eversmann@arch.ethz.ch*
[b] *TU Munich, Germany, andre.ihde@tum.de*
[c] *TU Delft, The Netherlands, Christian.Louter@tudelft.nl*

The fabrication of projects with complex geometries often implies a significant waste of material, since custom molds need to be created and irregular shapes need to be cut out of larger sized elements. For low curvatures, cold elastic bending processes can be applied. However, elastic bending techniques have mainly been utilized to create simple curvature panels for architectural projects. This paper explores computational simulation in relation to a digitally controlled fabrication method of bending rectangular glass sheets elastically into irregular double curvature. This is done through exploratory prototyping within the framework of a Master of Science course on digital production, and additional computational modeling and FE-analysis. We used algorithmic real-time simulation to approximate the bending process of cold-bent glass and elaborated on details of the simulation process and possible surface types and curvatures. Our empirical tests on simply curved, ruled and doubly curved surface types used float glass as well as heat-treated glass. A detailing system was developed to clamp the glass panels into position. We evaluated the results of the computational simulation (Rhino with plug-ins) as well as FE-Analysis (Strand 7) and compared the resulting geometries to the measurements of the physical prototypes. In order to demonstrate the system's capacities on a larger multi-panel geometry, we constructed a 5m x 4m prototype of a doubly-curved glass surface.

Keywords: cold bending, double curvature, particle-spring simulation, FE-analysis, digital fabrication

1. Introduction

Digital fabrication technologies are typically applied for projects with complex geometries in order to fabricate irregular geometry in a precise manner. Often subtractive fabrication processes are needed, resulting in a large waste of material. Custom mold geometry is costly to fabricate and needs to be stored afterwards to allow the reproduction of broken building parts. For low curvatures, elastic bending methods can at the same time enhance structural performance (Lienhard, 2014) and produce new architectural forms and effects. Intrinsic material properties can be simulated through computational methods to minimize material use and assembly effort for curved geometries.

However, elastic bending techniques have mainly been utilized to create simple curvature panels for architectural projects. For more complex surfaces, multiple simply curved panels can be combined to create larger surfaces, approximating double curvature (Eigensatz et al, 2010). In this approach, the panels need to be cut into irregular frame geometry.

The collaborative work presented in this paper builds on recent research and façade engineering, attempting to enlarge the elastic bending process to irregular surface geometry while taking into account real fabrication tolerances in relation to surface geometry and using standard-sized rectangular glass sheets as the base material. It combines the practical work on exploratory cold-bent glass prototypes realized in a Master of Science course on "Digital Design and Production" and additional computational simulation (Rhino and associated plug-ins) and FE-analysis (Strand7). The comparison between the measurements of the physical prototype, the computational simulation and the FE-analysis results validates the computational framework for a tolerance of 1-2mm, which is barely visible by the human eye. In order to demonstrate the system's capacities on a larger multi-panel geometry, we constructed a prototype of a 5m x 4m doubly curved surface. The paper evaluates the employed simulation and fabrication techniques and discusses their application for standard construction and future digital fabrication processes.

2. Cold-Bending of Glass

The traditional method of bending glass is by means of hot-bending techniques. This involves heating the glass and bending or sagging it into a single or double mold system. The disadvantages of the hot-molding technique are the high costs due to molding, high energy consumption, a risk of optical distortions, impracticable transportation of the worked piece and long delivery times, especially if later replacement is necessary (Belis et al., 2007). An interesting alternative is cold-bending of glass. This involves the elastic bending of glass by curving or warping a glass panel in

the desired curvature and subsequently fixing it to a rigid substructure. Alternatively, the curvature of cold bent glass can also be sustained through lamination techniques in which individual cold bent glass panels are bonded through adhesive interlayers (Fildhuth and Knippers, 2011). Recent developments in glass research and façade engineering underline the great potentials for applications of cold-bending in architecture (Beer 2015), (Belis 2009), (Datsiou & Overend 2014), (Eekhout & Niderehe 2009), (Feijen et al. 2012), (Fildhuth & Knippers 2011), (Raynaud 2014), (Teich et al. 2014), (Vollers 2004).

3. Double Curvature Glass Bending

3.1. Computational Simulation and Geometric Possibilities

We investigated two different approaches based on similar simulation modeling techniques. The first one was a form-finding approach in which forces act on the simulation model and produce an ideal geometric result. The second approach started from a given target geometry, which was approximated as close as possible by a simulation routine. For both approaches we used a particle-spring based modeling technique. This technology has been developed for advanced computer graphics and has been used to simulate physical behavior (Lienhardt, 2014). A high degree of interaction and integration into real-time design processes can be achieved (Kilian and Ochsendorf, 2005). Particle systems have not been used extensively for engineering purposes, but allow for user interaction during the analysis and provide a continuous structural feedback (Melgar, 2011). The major advantages of the physics based simulation are its speed and sufficient accuracy for the form generation. Finite Element (FE) analysis can produce more accurate results, although it is still rather time-consuming. The FE-analysis approach is discussed later in Section 3.3, and is compared with the results and the geometric measurements of the prototypes in Section 4.

There are many techniques with varying degrees of efficiency and stability to solve the equilibrium geometry of particle-spring systems. For our experiments, we used the Runge Kutta integration in the software plugin Kangaroo 0.99 (later processes also used version 2.0) for the CAD-modeling software Rhino. In the form-finding approach the glass sheet was modeled by a particle-spring system. Therefore, the glass surface was subdivided into a quadrilateral mesh with diagonal cross-bracing. The resolution of the subdivision could be altered even though the accuracy after a certain threshold is fairly resolution independent (Volino and Magnenat-Thalmann, 2006). Each of the mesh vertices can be seen as a lumped mass, called particle. The particles were then interconnected by linear springs. Each of the springs subsequently got assigned a constant axial stiffness, an initial length, and a damping coefficient. Calibration tests were effectuated on simple static systems to compare the deflection results of single span beams and cantilever girders in order to verify the specific settings and unit systems. The stiffness values S of the springs were calculated via Eq. (1).

$$S = \frac{\text{E (Young's Modulus in (N/mm}^2\text{)}\times\text{A (crosssection in mm}^2\text{)}}{\text{L (length in mm)}} \quad (1)$$

Additionally, a bending stiffness was applied between each of the continuous linear elements via K = E×I, where E is the Young's modulus in N/mm^2, and I is the second moment of area in mm^4.

The software uses an incremental dynamic relaxation method to formulate the bending energy adopted from Adriaenssens et al. (2001). The deforming bending forces apply only on the border of the glass fixation, therefore the mesh was modeled with a varying mesh cell size (Fig. 1a, low resolution). In the glass clamping detail described in section 3.2 and 5.3, the two opposing forces were created through the fixation screws pushing the panel downwards and the frame geometry pushing the glass panel upwards (Fig. 1b).

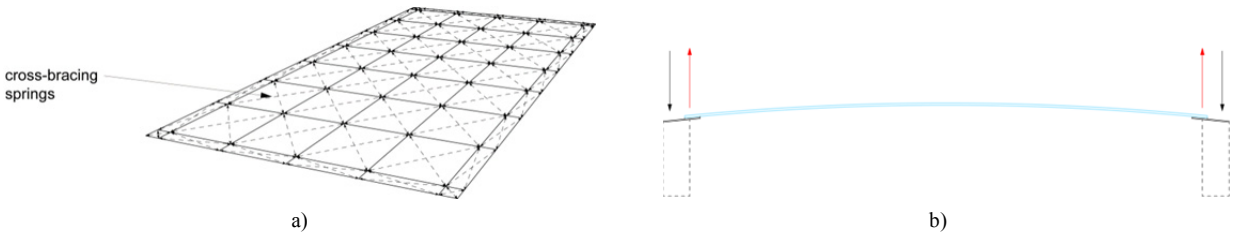

a) b)

Fig. 1a) Particle-Spring system b) Bending force vectors.

Now an external force was applied on one or multiple particles, causing all springs to readjust into a new state of equilibrium. When a force is applied, each of the springs tries to readjust its geometry, achieving the closest value to its initial length depending on its assigned stiffness. This can lead to various geometric results depending on the direction and value of the forces. Like bending a sheet of paper by hand, in order to achieve curvature, forces need to be applied from multiple positions simultaneously (Fig. 2).

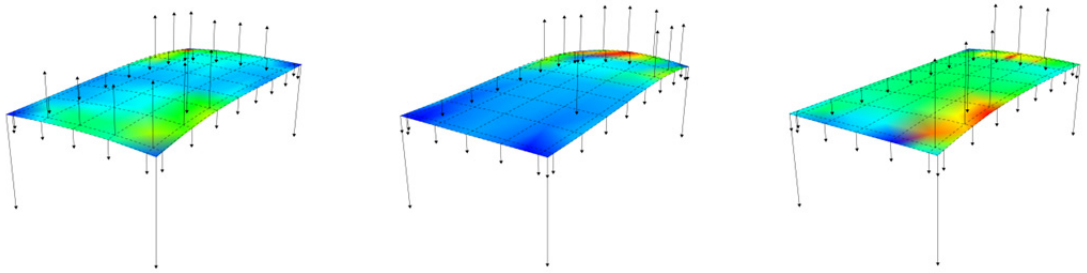

Fig. 2 Variable single sheet curvatures and applied bending force equilibrium.

This approach can be used efficiently if the surface is undefined by the designer and can be created to correspond to the applied forces. For architectural applications, this is however rarely the case since there usually are very specific surface requirements from the designer. Therefore we investigated a second approach. This approach started from a target surface, on which the system tried to approximate the bent geometry as close as possible. For this approach we extended the previously described particle-spring system. We added another set of springs in-between the initial flat glass sheet and the target geometry. The springs were modeled using force-density springs which can slowly increase their initial stiffness. These springs were programmed to contract to a length equaling zero (=0). The springs could slowly increase their force until reaching a final position as close as possible to the provided target geometry, while deforming the glass sheet within a safe elastic range. To make sure that the glass sheet was not bent more than the maximal stresses allow, the minimum curvature bending radius was calculated with Eq. (2).

$$r = \frac{E \times t}{2 \times \sigma} \tag{2}$$

Where: r radius in mm, E Young's Modulus in N/mm^2, t thickness of glass sheet in mm, σ maximum allowable stress in HSG in N/mm^2.

On a grid of points on the bent surface, the main curvature radii were calculated through evaluating the Gaussian curvature. The results were sorted by the smallest radius which was compared continuously through a feedback loop with the simulation. If the simulated surface got close to the minimum curvature radii, the force density springs ceased to increase their axial stiffness any further, therefore stopping the bending process. The target points of the force density springs were derived from a projection towards the normal vector of the target surface. These points were however not the final geometric position, since their final position had to be negotiated between the deformation stiffness of the glass sheet and the pull strength of the force density springs (Fig. 3).

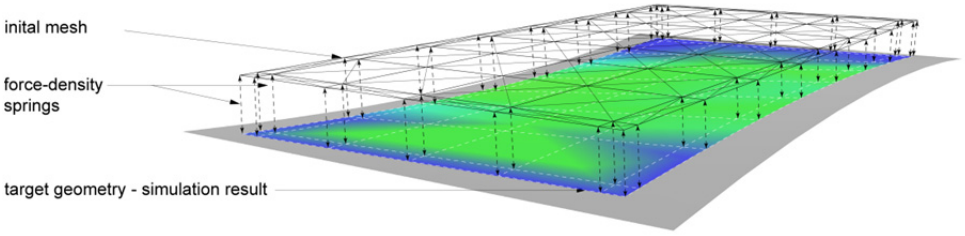

Fig. 3 Approximate bending on target geometry.

The system was tested on multiple surfaces of synclastic and anticlastic typology using target geometries of main curvature radii between 8m and 20m. Results show that in synclastic curvatures (Fig. 4a), the measured distances between the target geometry and simulation result were larger (up to 3mm difference) especially in the middle of the panel, where the curvature is flattening out. Anticlastic curvatures produced more precise results with around 0.6 mm of maximum difference (Fig. 4b,c).

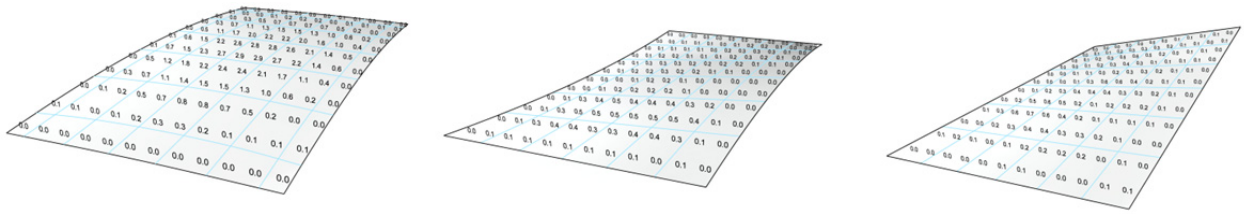

Fig. 4a), b), c) Tolerance measurements between target geometry and simulation result.

For a multi-panel geometry, the system also had to accommodate for small tolerances in-between the panels of variable curvatures. Therefore the tolerances of the joint in-between the panels was added using a third set of springs with a stiffness depending on the maximum allowed tolerance of the detailing system. These springs act similar to a stitched connection between textiles, allowing the glass sheets to move freely within a given range until they achieve their equilibrium state during simulation. This was tested again on various geometries. The surface continuity can be visually verified using a reflection line test described in Architectural Geometry, Pottmann et al (2009) (Fig. 5).

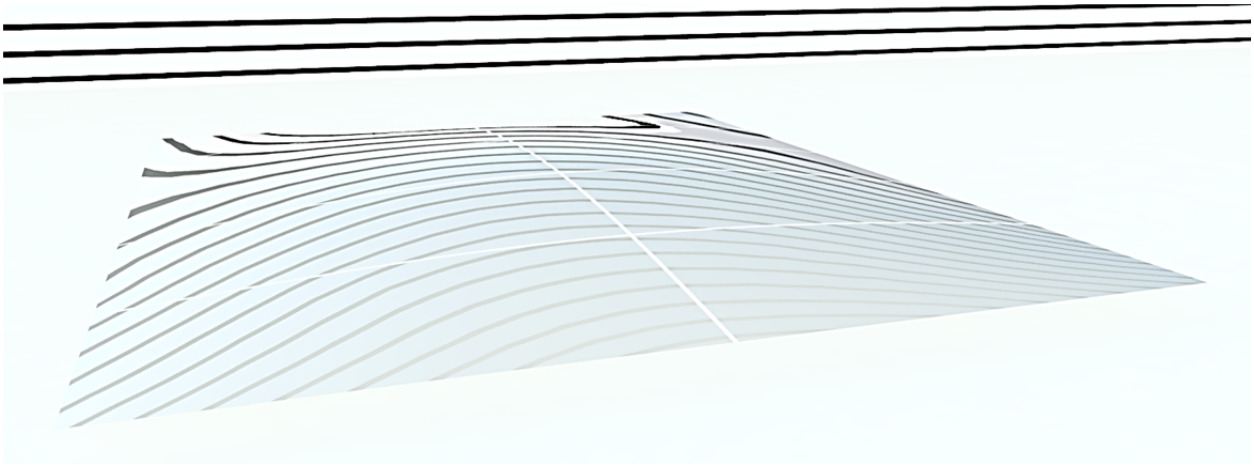

Fig. 5 Surface continuity of multiple sheet simulation.

3.2. Prototypes and Detailing

A first series of bending tests were performed using rectangular panels of 1.0 m x 2.0 m of standard 4 mm annealed float glass. The substructure, loading points and detailing technique were varied to achieve single and double curvature surfaces. As annealed float glass (ANG) has a relatively limited characteristic bending strength of 45 N/mm^2, compared to heat-strengthened glass (HSG) 70 N/mm^2 and fully tempered glass (FTG) 120 N/mm^2, HSG was used for doubly curved prototypes where higher bending stresses are expected. Also, annealed glass may suffer from stress-corrosion phenomena, whereas this is absent for heat-strengthened and fully tempered glass as long as the compressive pre-stress is not overcome.

For a single curvature surface, panels of plywood were digitally cut to a radius of 6.0 m and assembled with a distance holding element of a straight 1.0 m plywood panel. In order to apply a deformation to the glass panel, first one side was simply fixed to the flat side of the substructure by an aluminum profile with a rubber inlay to protect the glass edge. The open edge of the glass panel was then slowly bent over the wooden substructure to its final form and then fixed again mechanically as the first edge. As a result, tension loads apply on the fixation of the two flat edges while the curved panels are pressing the panel into its curved state (Fig. 6).

Fig. 6 Single curvature prototype.

While achieving a simply curved surface is relatively simple, forcing the material into double curvature is a more challenging method for the fabrication details of the structure as well as the bending process. For the sub-structure of the double curvature prototypes, panels of plywood were digitally cut using a Maka 5-axis CNC router to a double-curved surface geometry and assembled into a frame. To be able to force the glass sheet into double curvature, loads needed to be applied simultaneously on multiple points, to prevent the surface from "snapping" again into simple curvature. Therefore we developed a special detail system, which was able to bend and fixate the panels. For this aluminum sheets were cut with a custom geometry by a waterjet CNC machine. The aluminum sheets were then glued with 3M acrylic foam on the surface of the glass panels at a distance of around 10 mm from the glass edge. This provides a linear clamping at the edge of the glass and a simultaneous protection of the glass edge. The panel was then laid on the structure. Using a set of specific long screws, the panel was clamped through the precut holes in the aluminum sheets. The panel could afterwards slowly be bent into its final form by tightening the screws simultaneously. As a result, tension loads apply on the fixation of the load points along the glued aluminum profiles while the wooden substructure is pressing the panel into its curved state. Three prototypes of varying geometry and anticlastic and synclastic curvature were built and digitally measured. The first, anticlastic prototype had a doubly ruled surface typology, which means that the surface generating curves are lines in two directions (hyperbolic paraboloid). The saddle-shaped surface is of negative Gaussian curvature which means that the centers of the principle curvatures lie on opposing sides of the surface. This surface had minimal main curvature radii of 11.5 m and 11.9 m (Fig. 7).

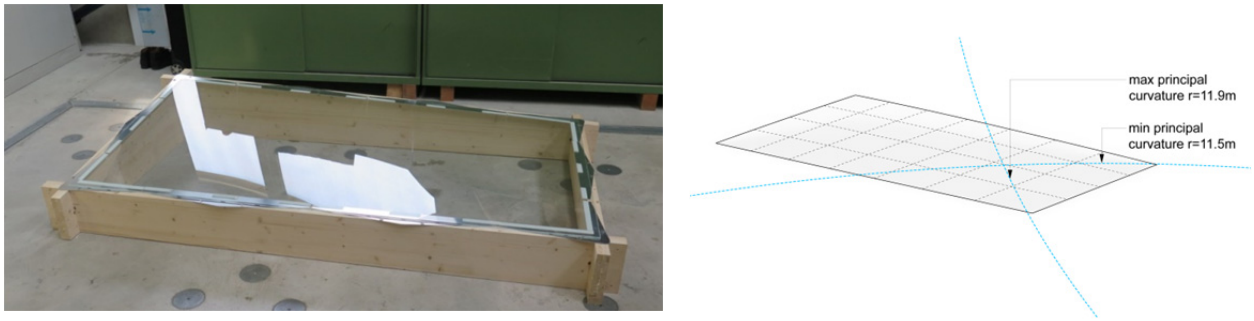

Fig. 7 Ruled-surface prototype.

The second prototype was of synclastic typology, which means that the Gaussian curvature is positive on all points and the centers of the principle curvatures lie on the same side of the surface. This surface had minimum main curvature radii of 6.5 m and 18.0 m. The wooden frame had side curvature radii of 8.6 m / 9.6 m (short/long side) (Fig. 8).

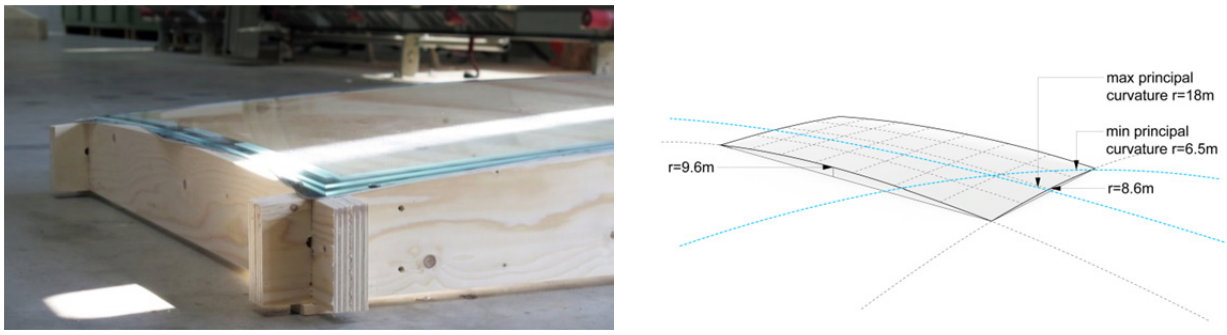

Fig. 8 First synclastic double-curvature prototype.

Since the last prototype was surprisingly easy to bend with few efforts, a third prototype of the same typology was built with the idea to realize a maximum of bending capacity. This surface had minimum main curvature radii of 4.0 m and 12.0 m. The wooden frame had side curvature radii of 6.1 m / 7.0 m (short/long side) (Fig. 9).

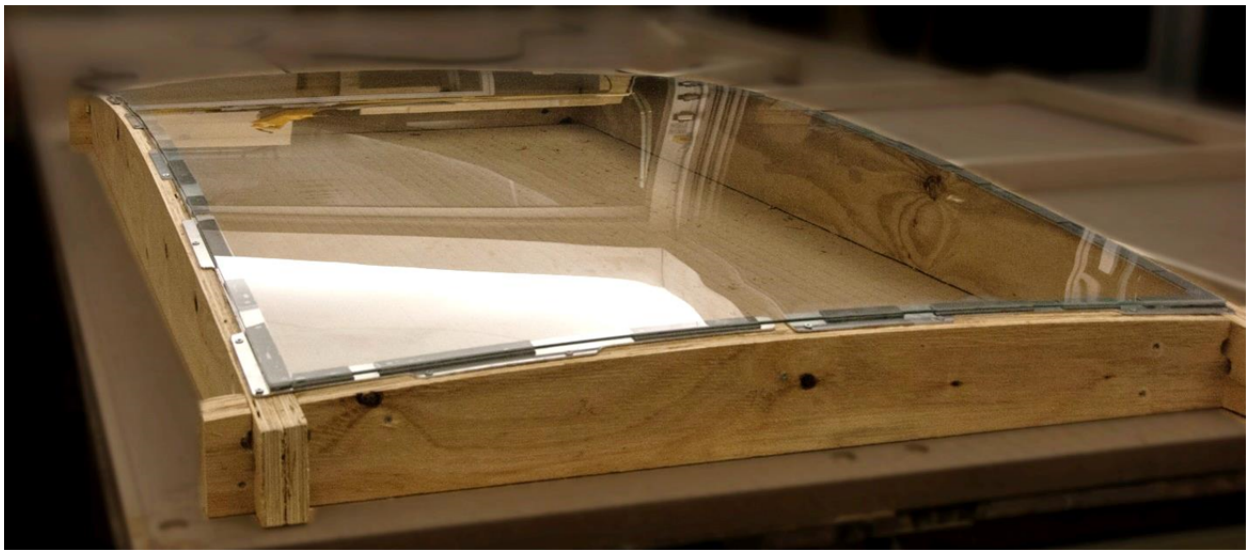

Fig. 9 Second synclastic double-curvature prototype.

3.3. Finite Element Simulation

The FE-analysis was performed with Strand7 (www.strand7.com) and had three objectives. The first objective was the verification of the resulting form of the computational simulation described in the section 3.1. The second aim was to enable a structural analysis of the bent glass, based on the principal stresses calculated in FE. The analysis of the structural behavior and material utilization with additional climate loads and a man load was defined as third goal. In addition, the FE results allowed a precise geometry comparison with the constructed prototypes described in section 3.2.

4. Base of the analysis and modeling

The following section describes the FE-analysis on the basis of the last double curvature prototype mentioned in section 3.2. A target geometry of minimum main curvature radii of 4.0 m and 12.0 m was used. The glass had the dimensions 1.0 m x 2.0 m. A glass panel of heat-strengthened glass of 4 mm thickness was used and 2 mm aluminum clamping strips were included in the model (Fig. 10).

The simulation started with the flat initial shape. The glass pane was then bent into the target position with the aid of bearing movements at 40 different points. For this simulation, the theory of third order (large displacement calculations, equilibrium at the deformed system) was used and the support movements were applied in incremental stages. Here, the self-weight of the glass sheet and the aluminum border elements were taken into account.

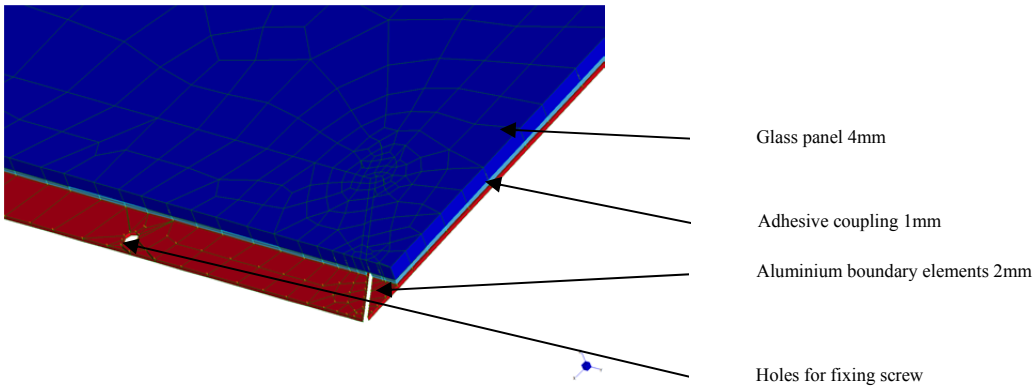

Fig. 10 FE Detail Modelling.

Both the aluminum elements and the glass sheet were represented as shell elements. For viscoelastic coupling between glass and aluminum, brick elements based on the rheological Mooney-Rivley model were applied. At the end of the assembly process, the timber substructure acts as a non-linear compression-only support. This additional support conditions were taken into account using the internal Strand7 stage manager. In this state beam, elements simulating the screws were included in the analysis.

The relevant principal stresses σ_{11} in the bent and fixed state can be found in Figure 11. With a maximum of 67 N/mm^2, the stress was close to the characteristic bending strength of the applied heat-strengthened glass. Taking into account partial factors (not included in the characteristics bending strength value), this configuration would not be applicable in real-world applications, and one would better convert to fully tempered glass. However, for the sake of this exploratory prototype the glass was able to sustain the curvature.

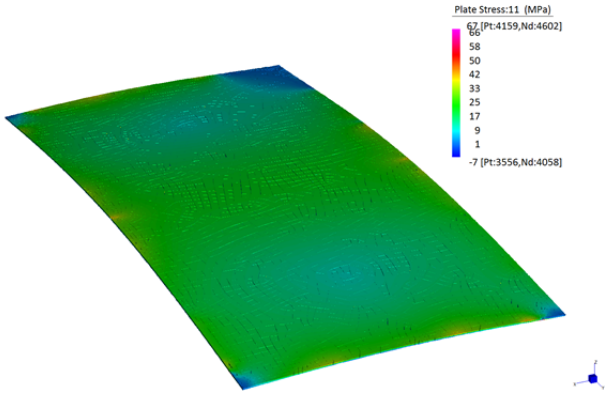

Fig. 11 Main stresses after bending.

In (Nicklisch 2010) the design stress for HSG (including partial factors) is given to be 29 N/mm^2. Taken into account this stress level as an upper limit, it can be seen from Figure 12a that this stress is exceeded at a few areas, especially at the perimeter of the glass where the clamping of the glass occurs. It should be mentioned, however, that both the exact connection between aluminum to glass as well as the shape of the aluminum elements were not yet fully optimized. Here we expect more optimized results in ongoing research. Figure 12b shows the contact stresses of the aluminum elements with the wooden substructure.

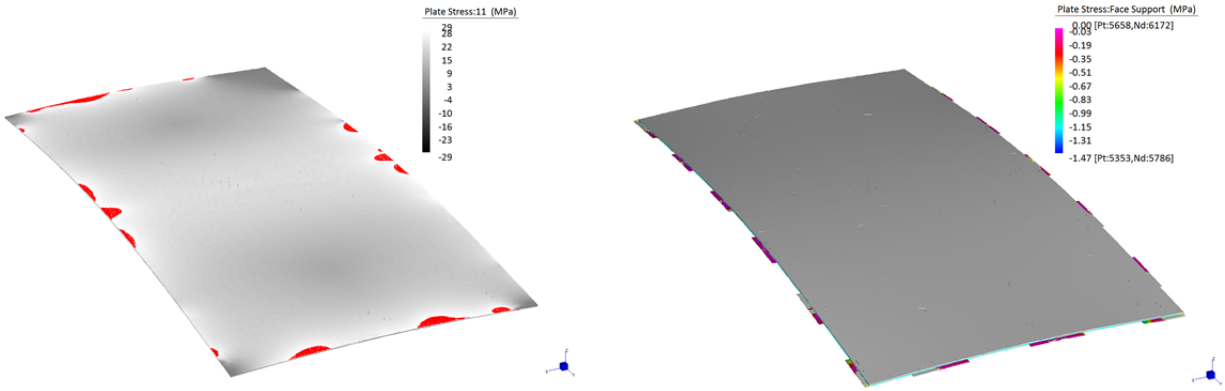

Fig. 12a) exceeding of maximum design stresses, Fig. 12b) contact stresses at the timber supports.

In a further analysis a surface load of 1 kN/m² (wind suction) was transferred to the glass pane. Here only a slight change in stress distribution compared to self-weight could be determined (Fig. 13a). The maximum relative deformation to the self-weight was 1.4 mm (Fig. 13b)

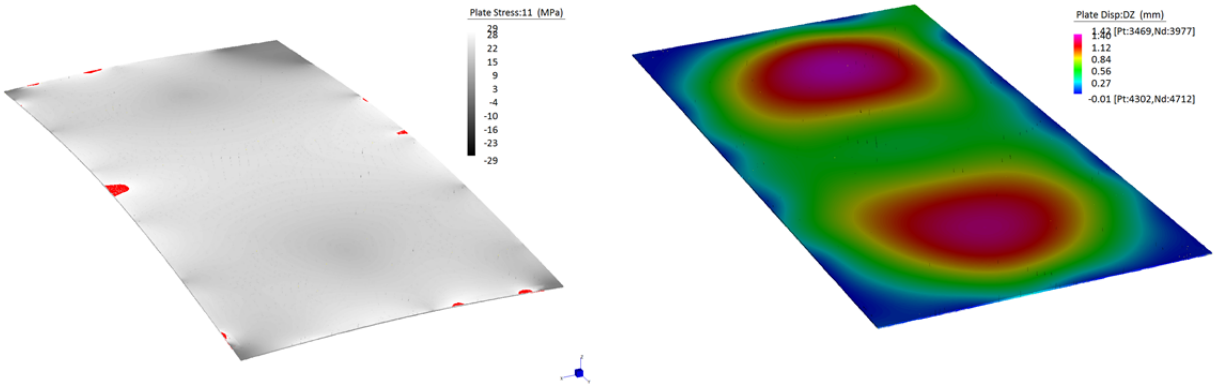

Fig. 13a) exceeding of maximum design stresses under wind suction, Fig. 13b) relative deflections under wind suction.

For snow loads (1 kN/m²) the stresses exceeded the 29 N/mm^2 in larger areas, but the tensions remained under 70 MPa of the characteristic value. A presumable failure of the HSG pane would occur under a central man load of 1 kN (≈100 kg). Tensions exceeded the allowable characteristic stress of 70 N/mm^2. This was accompanied by relative deformations of up to 14 mm (Fig. 14).

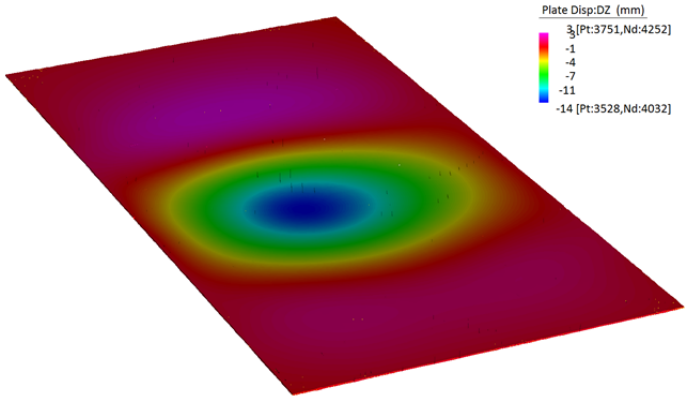

Fig. 14 Central man load.

5. Remarks to FE-analysis

To summarize the results of the FE-analysis, the following statements can be made:

- The HSG panel could withstand the bending process as well as the wind and snow loads considering a design stress of 29 N/mm^2.
- A verification following an Ultimate Limit State (ULS) was not successful with HSG and the current thickness of the glass pane.
- Significant overstressing occurred under man load, so load distributions are necessary.

6. Comparison Computational Simulation – FE-Simulation - Prototype

In order to evaluate the geometric results of the computational simulation model and the FE-analysis, the double-curvature prototype described in Section 3.3 was precisely measured. A regular grid of 40 points was projected on the model and measured via a laser distance sensor. The points were marked on the glass surface with non-reflective tape for a precise measurement. The linear laser sensor could then follow the point grid through 2-dimensional controlled movement and take the measurements in the vertical direction (Fig. 15a).

The comparison between the measurements and the computational simulation described in section 3.1 shows that the geometry of the prototype in the middle parts is slightly less curved than in the computational simulation (Fig. 15b). Also the corners are slightly less bent than in simulation, which could be caused by the fixation distances of the screws. This is especially visible in the right corner in the back, where fixation occurs offset from the corner to allow a next panel to interlock. The measurements in comparison to the FE-analysis are more evenly distributed and show a slightly better precision (Fig. 15c).

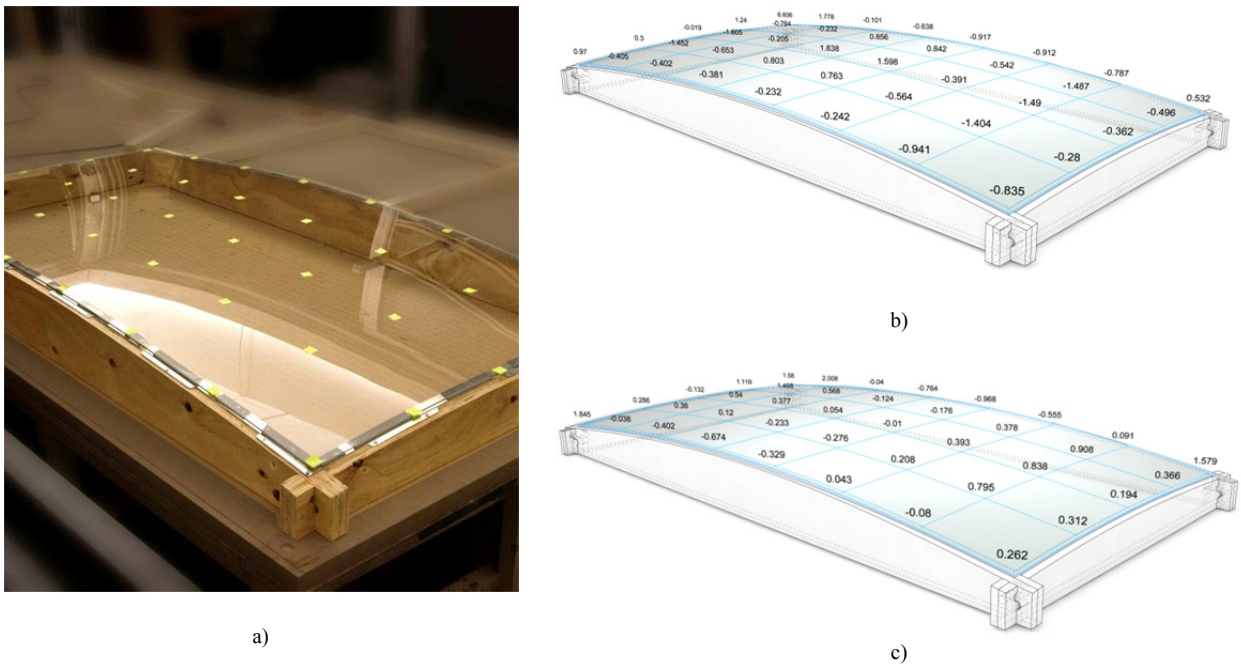

a) b) c)

Fig. 15 Laser measuring a) Setup b) Physical Simulation c) FE-analysis; differences in mm.

The comparison shows that the physical simulation tool can be effectively used as a form finding method with a precision up to 1-2 mm. For a calculation of bending stresses and a more precise geometric definition, the slower FE-analysis is necessary.

7. Demonstrator Project

In order to show the system's capacities on multi-panel doubly curved surfaces we constructed a demonstrator of a 5.0 m x 4.0 m doubly curved surface consisting of 10 rectangular 1.0 m by 2.0 m edge treated HSG panels of 4 mm thickness (Fig. 16).

Fig. 16 Demonstrator project.

7.1. Surface Geometry

This prototype followed the first approach of simulation as described in Section 3.1 to define the overall geometry of all 10 panels. This target geometry of the panels was created in a lower mesh resolution through applying simultaneously an upwards directed force on the interior grid points, while a second force presses the outer edge on the ground. This resulted in an almost rectangular shape in plan, diverging 1.8 mm/ 6.8 mm in the midpoints of the edges. The overall surface had 10 panels of varying double curvature. Afterwards, the bending of each of the panels was calculated using the second physical simulation process described in section 3.1. The simulated panels had a maximum deflection of 3 mm from the target surface geometry and the joint width had a tolerance of maximum 2.3 mm (Fig. 17).

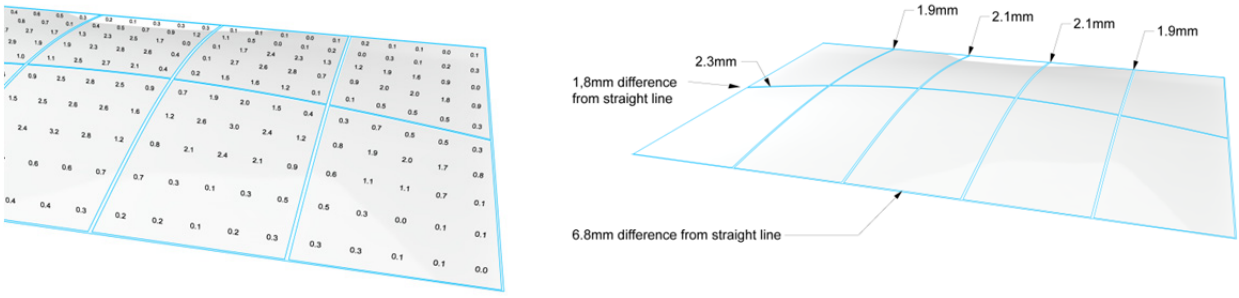

Fig. 17 Simulation tolerances a) to target surface b) open joint maximum tolerances.

7.2. Structure

The structure was composed out of a rectangular frame supported by 14 temporary foundations. A grid of cross and transversal beams formed the sub-structure of the glass panels. The beams were fabricated out of three layers of 21mm plywood, which were fixated by screwing. Glass and aluminium frames acted as horizontal stiffeners.

7.3. Detailing Approach

With glass as material, detailing becomes a central issue, since the borders of the glass are the most fragile part of the material. A detailing system was developed to apply forces into the plane of the glass surface rather than the edges. Therefore a custom waterjet-cut aluminum profile was glued with a distance to the edge onto the inner surface of the glass plates. The shape of the aluminum profile allowed adjacent panels to interlock, keeping the screws of two neighboring plates almost in a central line to the beam (Fig. 18).

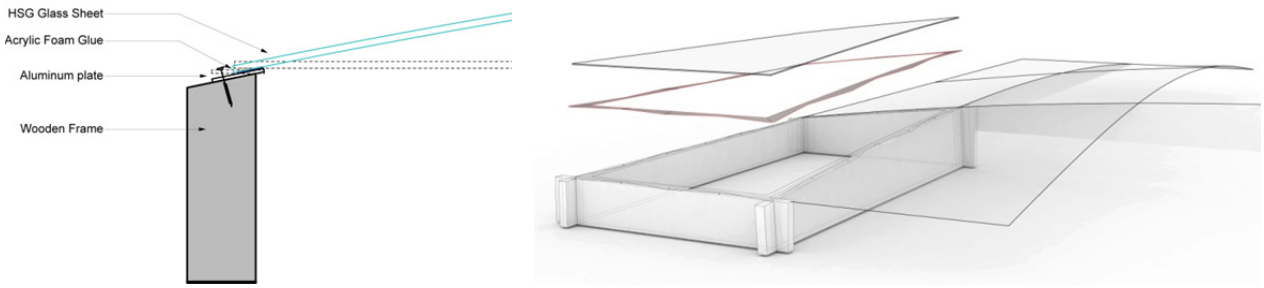

Fig. 18 Detail and bending assembly.

The joint width could be minimized to 20 mm. The human eye can perceive joint misalignments well up to 2-3 mm of tolerance, while values below remain largely unnoticed. The realized large-scale demonstrator project shows that the tolerances are barely noticeable (Fig. 19). The gaps between the panels could be covered by silicon joints to ensure water tightness.

Fig. 19 Detailing system.

8. Discussion

The physical simulation system is capable of simulating double curvature bending of various geometries. Specifically developed computational framework allows form finding and the generation of fabrication data. The comparison between the measurements of the physical prototype and the computational simulation and the FE-analysis results validates the computational framework for a precision of up to 1-2mm. For the analysis of bending stresses and variable load tests of the glass sheet, FE-analysis has to be effectuated.

Maximum stresses occur not necessarily in the areas of most important curvature, but at specific points close to the fixation of the aluminum plates and screw holes. Further research needs to be done in order to optimize the geometry of the fixation system, its fixation rhythm and position. Peak stresses might also be occurring through the continuity of the acrylic foam adhesive tape between the plates and the glass sheet which is applied in flat state, and which may cause stress due to thermal expansion differences.

When using curved glass elements in a grid shell structure, it must be ensured that the glass panels are decoupled from the load transfer of the overall construction, since this can cause additional stress. Should such a bent panel be also used as stiffening element, extensive considerations for redundancy of the overall structure must be taken into account in case of failure of individual panels. The influence of constructive implementation would have to be studied further. In this case, it would be conceivable to add elements which allow the structural integrity of the overall construction to be sustained until a broken glass pane can be replaced. Also, when applying glass in overhead conditions, typically laminated glass is required to prevent human injury upon glass fracture.

Finally, it should be noted that the construction of the physical prototypes and demonstrator was done within the framework of a Master of Science course on "Digital Design and Production". The choice of glass was highly influenced by practical considerations such as delivery times and available budgets. Therefore, the glass types are not directly in line with requirements set in the building industry, but nevertheless provide a good insight into the cold-bending techniques within these exploratory prototypes.

9. Outlook

The bending procedure and detailing system could be fabricated at a reasonable cost. While non-standard metal sheet cutting for the connecting plates is widely available, 5-axis CNC routing necessary for the wood frame geometry is still considered as quite specific fabrication equipment. Fabrication alternatives using elastic bending processes also for the framework could be subject of future research. Collaborative robotic fabrication methods could allow high precision bending and fixation procedures.

Bending the glass panels on site has the clear advantage that the sheets can be delivered flat, reducing delivery costs drastically. Prefabricated elements as for unitized curtain-walls have the advantage of a greater fabrication precision and reduction of assembly time on the construction site. The recent developments of on-site robotic fabrication techniques at the NCCR Digital Fabrication at ETH Zurich suggest a change in these opposing arguments, bringing high precision fabrication techniques also on construction sites.

Finally, it should be noted that the current paper uses single glass panels only, as set by the boundary conditions of the MSc course. For standard construction applications often laminated glass (LG) and/or insulating glass units (IGU) are required. For cold-bending applications, these glass configurations bring along additional complexities, such as the visco-elastic response of the interlayer (for LG) and the durability of the stressed cavity sealant (for IGU). Issues regarding cold-bent laminated glass are addressed in other studies, such as (Belis, 2007), (Fildhuth, 2011), (Galuppi & Royer-Carfagni 2015) and others. Geometric possibilities of the cold-bending of twisted IGUs have been also studied by (Laufs et al, 2010), (Beer, 2015) and others.

Acknowledgements

The physical prototypes and the demonstrator project have been developed and constructed during a Master's elective course at EPF Lausanne held in collaboration between Philipp Eversmann, Paul Ehret, Christian Louter, Manuel Santarsiero and the students Andrea Baraggia, Dominik Baumann, Tomas Odelbo, Agnes Ulrika Charlotta Orstadius, Francesca Rabbiosi, Itai Vander, Robbert Verheij and David Viladomiu Ceballos.

References

Adriaenssens, S.M.L., M.R. Barnes: Tensegrity spline beam and grid shell structures, Engineering Structures 23 (2001) p. 29–36

Beer, B.: "Complex Geometry Facades – Introducing a New Design Concept for Cold-Bent Glass", Glass Performance Days, Finland, 2009

Beer, B.: Structural Silicone Sealed Cold-Bent Glass – High-Rise Projects Experience Leading to a New Design Concept, Glass Performance Days 2015, pages 235-240, 2015

Belis, J., Inghelbrecht, B., Van Impe, R., Callewaert, D.: "Cold bending of laminated glass panels", HERON Vol. 52 (2007) No. 1/2½

Datsiou, K.G., Overend, M., Behaviour of cold bent glass plates during the shaping process, Engineered Transparency conference 2014, Dusseldorf, Germany, pages 125-133, 2014

Eekhout, M., Niderehe, S.: The new, cold-bent glass roof of the Victoria & Albert Museum, London, Glass Performance Days, Finland, 2009

Eigensatz, M., Kilian, M., Schiftner, A., Mitra, N., Pottmann, H., Pauly, M.: „Paneling Architectural Freeform Surfaces", ACM Trans. Graphics, 29/4, #45, Proc. SIGGRAPH (2010)

Feijen, Vrouwe, I., Thun, P.: „Bent Single Curved Glass; Opportunities and Challenges in Freeform Facades", Challenging Glass 3 – Conference on Architectural and Structural Applications of Glass, TU Delft, June 2012

Fildhuth, T.,, Knippers, J.: „Geometrie und Tragverhalten von doppelt gekrümmten Ganzglasschalen aus kalt verformten Glaslaminaten". Ernst & Sohn, Stahlbau Spezial 2011 – Glasbau/Glass in Building

Galuppi, L., Royer-Carfagni, G.,, Optimal cold bending of laminated glass, International Journal of Solids and Structures, Volumes 67–68, 15 August 2015, Pages 231-243

Kangaroo. [Online]. http://www.grasshopper3d.com/group/kangaroo

Kilian, A., Ochsendorf, J.: "Particle-spring systems for structural form finding", journal of the international association for shell and spatial structures: IASS, 2005

Laufs, W., Vilkner, G.: „Gekrümmte Glasflächen – Zusammenspiel von Geometrie und Glasdetaillierung", Stahlbau Spezial (March 2010)

Lienhard, J.: „Bending-Active Structures", Institut für Tragkonstruktionen und Konstruktives Entwerfen der Universität Stuttgart, Forschungsbericht 36, 2014

Melgar, E.R.: "Integrating Physics into the Design Process" Thesis, Bartlett School of Graduate Studies, University College London, September 2011

Nicklisch, F., Thieme, S., Weimar, T., Weller, B.: "Konstruktion und Bemessung Vertikal- und Überkopfverglasungen, Absturzsichere Verglasungen, Begehbare Verglasungen", Glasbau-Praxis: Berechnungshilfen Broschiert (2010) p. 295

Pottmann, H., Asperl, A., Hofer, M. and Kilian, A.: "Architectural Geometry", Bentley Institute Press (2007)

Rhinoceros. [Online]. http://www.rhino3d.com

Teich, M., Kloker, S., Baumann, H.: Curved glass: bending and applications, Engineered Transparency conference 2014, Dusseldorf, Germany, pages 75-83, 2014

Volino, P., Magnenat-Thalmann, N.: "Simple Linear Bending Stiffness in Particle Systems" Eurographics/ ACM SIGGRAPH Symposium on Computer Animation (2006)

Vollers, K.: „Usage of Cold Bent Glass Panes as an Approximation for Doublecurved Surfaces", CTBUH Seoul Conference, 2004